COMMUNICATION

# Basic $[Au_{25}(SCH_2CH_2Py)_{18}]^-\cdot Na^+$ Clusters: Synthesis, Layered Crystallographic Arrangement, and Unique Surface Protonation

Zhong Huang, Yohei Ishida,* and Tetsu Yonezawa*

**Abstract:** We report the first synthesis of high-purity and high-yield $Au_{25}$ clusters protected by the basic pyridyl ethanethiol ($HSCH_2CH_2Py$, 4-PyET and 2-PyET). Single-crystal X-ray diffraction of the $[Au_{25}(4\text{-}PyET)_{18}]^-\cdot Na^+$ clusters has revealed a structure similar to that known for the phenyl ethanethiolate analog, but with pyridyl-N coordination to $Na^+$, a more relaxed ligand shell, and a profoundly layered arrangement in the solid state. Because of the pendant Py moiety, the $[Au_{25}(4\text{-}PyET)_{18}]^-$ clusters are endowed with a unique (de)protonation equilibria, which has been characterized in detail by UV-vis absorption and $^1$H-NMR spectroscopy. $[Au_{25}(4\text{-}PyET)_{18}]^-$ clusters showed an unexpectedly $H^+$-dependent solubility that is tunable in aqueous and organic solvents. The successful synthesis of the basic Py-terminated thiolate-protected $Au_{25}$ clusters paves the way to realize a new family of metalloid clusters possessing basic properties.

Thiolate-protected metalloid gold clusters ($Au_m(SR)_n$) with atomic precision and diverse structures have gained increasing attention in research owing to their intriguing physicochemical properties,[1] which facilitate their potential application in many contexts such as catalysis,[2] sensing,[3] and bioapplications.[4] Several studies have highlighted the importance of using SR ligands for metal clusters.[5,6] The R-group variability on the clusters is of great importance, not only in the "survival of the fittest" of target NC formation,[5] but also in the rational design of their functional properties and applications.[6]

Regarding the acidity/basicity, or the R-group's (de)protonation state in solution, a variety of $Au_n(SR)_m$ clusters have been prepared using SR ligands containing neutral (e.g., 2-phenylethanethiol, benzylmecaptan, methylbenzenethiol, alkanethiols, and adamantanethiolate), acidic (e.g., mercaptocarboxylic acids, mercaptobenzoic acids, and captopril), and both acidic and basic groups (e.g., glutathione, L-cysteine, and DL-homocysteine).[1–6] To the best of our knowledge, only three reports have been published for basic R-groups. In 2012, $Au_{25}$ cluster stabilized by 4-aminothiophenol ($HSPhNH_2$) was prepared but its molecular formula was assigned as $Au_{25}(SPhNH_2)_{17}$.[7a] In 2014, Xie *et al.*[7b] developed a NaOH-mediated $NaBH_4$ reduction method for $Au_{25}$ NC synthesis using cystamine ($HSCH_2CH_2NH_2$). However, cystamine interacts with mercaptocarboxylic acids for stabilizing the $Au_{25}$ clusters and therefore pure basic cystamine-capped $Au_{25}$ was not obtained. The latest reports by Whetten *et al.*[7c,d] released the earlier evidence of polydisperse captamino ($-S(CH_2)_2N(CH_3)_2$)-capped Au clusters with atom numbers ranging from 25–144. These few works seemed to confirm a statement made in 2005: “Small positively charged ligands do not support the production of “monolayer protected clusters” (MPCs) in the Brust synthesis”.[6c] However, the amino-terminated Au clusters would offer great advantages in (i) “make MPCs behave like proteins”,[7c,d] which envisions the possibility to analyze them using modern standard techniques utilized in molecular biology developed steadily over more than a half-century, and (ii) biological applications in which the amino-moiety incorporated on nanoparticle surface caters a long-held belief that it yields intimate interactions with the negatively charged contents.[4] In our recent works,[8] the modified Brust method at an optimized reduction rate could successfully synthesize $Au_{25}$ clusters utilizing a SR ligand with the pendant quaternary-ammonium group $-[N(CH_3)_3]^+$.

**Scheme 1.** Molecular structures of 4-PyET, 2-PyET, and PET thiols.

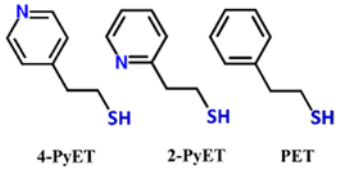


In this work, for the first time, we demonstrate that the pyridyl ethanethiol $HSCH_2CH_2Py$ (4-PyET or 2-PyET, Scheme 1) can be employed in Au cluster synthesis. The N center of the Py-group features a lone pair of $sp^2$ electrons; consequently, PyET is basic, similar to the tertiary amine. The synthesis of $[Au_{25}(4\text{-}PyET)_{18}]^-$ clusters was carried out using a technique similar to the typical synthetic strategy (see the Experimental section in Supporting information) for preparing $Au_{25}$ clusters[9] with the exception of using a THF–MeOH solvent mixture instead of the commonly used THF, MeOH, or $H_2O$.[6,7,9] PyET shows good solubility in $H_2O$ and MeOH but is only slightly soluble in THF. We first attempted a series of syntheses in the single solvents $H_2O$, MeOH, and THF. It was seen under $NaBH_4$ injection that the use of MeOH formed Au nanoparticles immediately and $H_2O$ led to the formation of polydisperse $Au_m$ clusters, but failed to achieve size-focusing of $Au_{25}$ clusters in the subsequent etching process (Figure S1). In contrast, the use of THF could facilitate the growth of monodisperse $Au_{25}$ clusters but its low solubility limited the production of clusters. Based on this, we proposed use of the solvent mixture, and THF–MeOH in a volume ratio of 3:1 was found to be perform the best in terms of the kinetically controlled growth of $[Au_{25}(PyET)_{18}]^-$ clusters (Figure S2), which would offer a new idea on building the comfortable environment for survival of monodispersed cluster, especially in cases of basic SR ligands. Although PyET is different from PET by substitution of only one

[a] Z. Huang, Dr. Y. Ishida, Prof. T. Yonezawa
Division of Materials Science and Engineering, Faculty of Engineering, Hokkaido University
Sapporo, Hokkaido 060–8628 (Japan)
E-mail: ishida-yohei@eng.hokudai.ac.jp
tetsu@eng.hokudai.ac.jp

Supporting information for this article is given via a link at the end of the document.

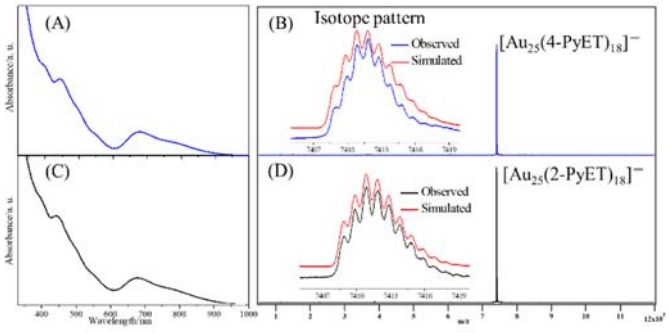


**Figure 1.** UV-vis absorption and negative-mode ESI mass spectra of purified $Au_{25}$ clusters: (A, B) $[Au_{25}(4\text{-PyET})_{18}]^-$ and (C, D) $[Au_{25}(2\text{-PyET})_{18}]^-$ (The insets show corresponding isotope patterns for the observed and simulated spectra).

CH group by N (Scheme 1), the solubilities of $Au_{25}$ clusters by the two species were significantly different. We therefore developed a new purification strategy for $[Au_{25}(4\text{-PyET})_{18}]^-$ clusters based on the protonation states of the pendant PyET ligands.

The UV-vis absorption spectra of the as-purified products both showed three distinct absorption bands at ~670, 450, and 400 nm and two weak absorption bands at ~560 and 780 nm (Figures 1A and C), which represent the typical spectroscopic fingerprints of SR-protected $Au_{25}$ clusters with a core charge of −1.[9] Negative-mode ESI-MS of the purified products showed only one peak at *m/z* ~7411.97, corresponding to $[Au_{25}(PyET)_{18}]^-$, for both 4-PyET and 2-PyET. The charge state (−1) of $Au_{25}$ clusters was confirmed by the characteristic peak separations of *m/z* ~1.00 and the molecular formula of $[Au_{25}(4\text{-PyET})_{18}]^-$ was validated by matching the observed isotopic patterns with the simulated ones (Figures 1B and D). Moreover, the positive-mode ESI-MS of both $[Au_{25}(4\text{-PyET})_{18}]^-$ and $[Au_{25}(2\text{-PyET})_{18}]^-$ clusters detected predominant peaks of $[Au_{25}(PyET)_{18}Na_x]^{x-1}$ (Figure S3), suggesting the counterions of $Au_{25}$ clusters should be $Na^+$ cations, which may coordinate strongly to pendant Py-groups via the N-atom's lone pair of electrons. TGA (Figure S4) revealed weight losses of ~33.9% and ~33.7% for $[Au_{25}(4\text{-PyET})_{18}]^-{\cdot}Na^+$ and $[Au_{25}(2\text{-PyET})_{18}]^-{\cdot}Na^+$, respectively, which are both very close to the theoretical loss of 33.8%. The yields of the final $[Au_{25}(4\text{-PyET})_{18}]^-{\cdot}Na^+$ and $[Au_{25}(2\text{-PyET})_{18}]^-{\cdot}Na^+$ clusters were calculated to be ~30% and ~35%, respectively, on the basis of Au atom content.

Single-crystal X-ray diffractometry (SC-XRD) measurements were acquired for $[Au_{25}(4\text{-PyET})_{18}]^-{\cdot}Na^+$ clusters (Figure S5,Table S1 and S2). Figure 2A depicts the overall crystal structure of the entire clusters, which is consistent with the ESI-MS formula (Figures 1 and S3), TG profile (Figure S4) and EDX measurment (Fiugre S6). Notably, the $Na^+$ cations and core anion showed $Na^+{\cdots}$"N" (−C5H5N) interactions (2.59 Å), similar to metal ion complexation.[10] The internal structure of $[Au_{25}(4\text{-PyET})_{18}]^-$ resembled that of previously reported $[Au_{25}(PET)_{18}]^-$ (as suggested by Figure S7).[9b,e] It showed an icosahedral $Au_{13}$ kernel that was capped by six pairs of $Au_2(4\text{-PyET})_3$ staple motifs to constitute an overall core–shell configuration (Figure 2B). As shown in Figure 2C, the Au–Au distances in the $Au_{13}$ core (bonds I and II) and the Au–S distances from the surface $Au_2S_3$ motifs (bonds IV and V) were almost identical regardless of the capped 4-PyET and PET ligands (Table S3), which could be rationalized by their analogous structures. However, the average core surface Au–motif Au distances (bond III, 3.18 Å) in $[Au_{25}(4\text{-PyET})_{18}]^-$ was

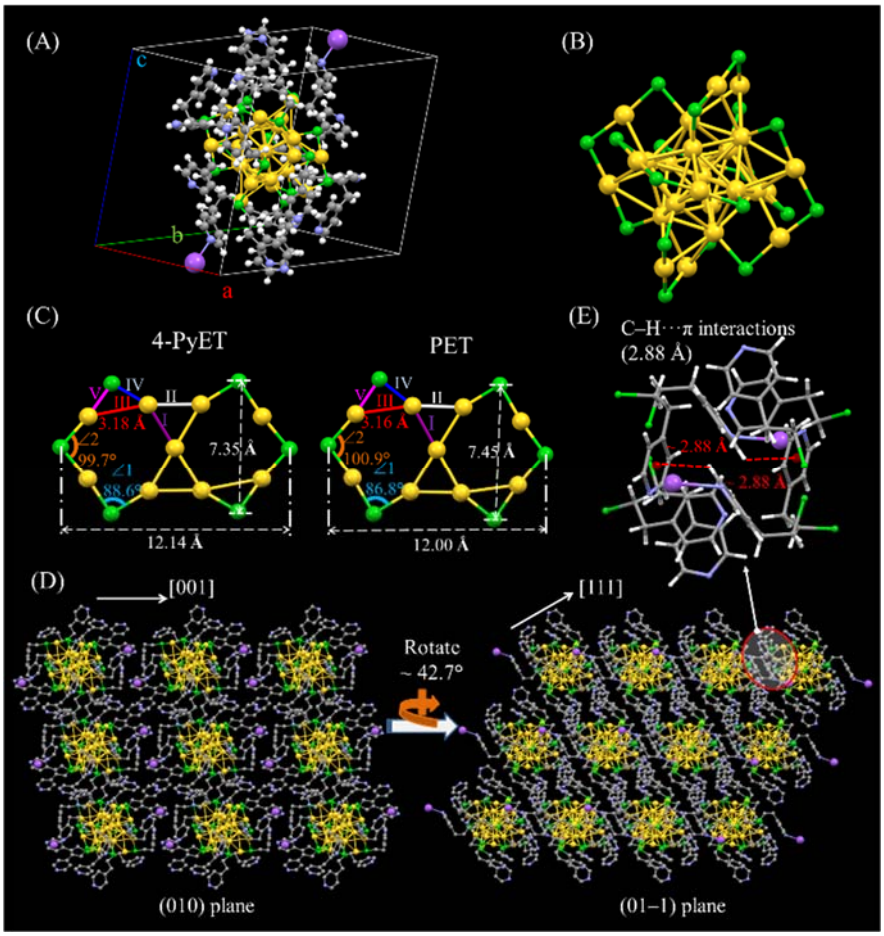


**Figure 2.** X-ray atomic structure of the $[Au_{25}(4\text{-PyET})_{18}]^-{\cdot}Na^+$ clusters: (A) overall structure—one disordered 4-PyET ligand and solvent molecules are removed for clarity; (B) $Au_{25}S_{18}$ skeleton of $[Au_{25}(4\text{-PyET})_{18}]^-$; (C) $Au_2S_3$ staple motifs along $\sigma_h$ planes of $Au_{25}$ clusters capped by 4-PyET and PET ligands. Bond types: I, purple, core Au–core surface Au; II, white, core surface Au–core surface Au; III, red, core surface Au–motif Au; IV, blue, core surface Au–motif S; V: magenta, motif Au–motif S. Bond angles: ∠1, light blue, ∠Au-S-Au—12 S atoms connected to one stapled gold atom and one gold atom vertex; ∠2: orange, ∠Au-S-Au—6 S atoms connected to two stapled gold atoms. (D) Views of 3×3×3 superlattice along (010) and (01–1) planes; H atoms are omitted for clarity. (E) C–H···π interactions between adjacent layers; ligands are shown in wireframe mode for clarity. Legend: yellow, Au; green, S; grey, C; blue, N; white, H; magenta, Na.

slightly longer than that in $[Au_{25}(PET)_{18}]^-$ (3.16 Å). In addition, the two types of ∠Au–S–Au angles in $Au_2S_3$ motifs showed obvious distinctions (∠1: 88.6° for 4-PyET against 86.8° for PET; ∠2: 99.7° for 4-PyET against 100.9° for PET). The changes led to an apparent extension of the exterior ligand shell along the $\sigma_h$ planes in $[Au_{25}(4\text{-}PyET)_{18}]^-$ clusters, as suggested by the increased diameter of the core structure (9.84 Å for 4-PyET against 9.78 Å for PET; see Table S3 and Figure S8) and the expanded average distances of the paired topmost S–S (12.14 Å for 4-PyET against 12.00 Å for PET) and squeezed average distances of the paired proximal S–S (7.35 Å for 4-PyET against 7.45 Å for PET) in the $Au_2(4\text{-}PyET)_3$ motifs. It seems reasonable to conclude that these changes were in response to the alternation of counterions from $TOA^+$ to $Na^+$. The smaller $Na^+$ cation should offer negligible steric effects to the atomic arrangement, resulting in a more relaxed ligand shell than that neutralized by the bulky $TOA^+$ cation.

More interestingly, $[Au_{25}(4\text{-}PyET)_{18}]^-\cdot Na^+$ clusters adopted a closest packing, and a very unique layered stacking sequence was found for its single crystal, as presented in Figure 2D. The ionic interactions between the $Au_{25}^-$ core and $Na^+$ cations generated two zones within adjacent unit cells (along the [001] direction), similar to that in the $[Au_{25}(PET)_{18}]^-\cdot TOA^+$ crystal (Figure S9).[9e] Moreover, along the (010) plane, after every $[Au_{25}(4\text{-}PyET)_{18}]^-\cdot Na^+$ species rotated clockwise (42.7°) along the b axis, the arrangement of clusters in single crystals represented that of a layered structure in the [111] direction. Intramolecularly and owing to the symmetry of overall structure (Figure 2a), the ligand shell also shows an inversion symmetry. The surface ligands could be divided into two groups, one of the paired $Na^+$-binding ligands and other sixteen of almost identical ligands that form a "ring" capping the core of cluster, as shown in Figure S10. Notably, the $Na^+$-binding ethylpyridyl thiolate substituents feature the inclination to enter its adjacent layers. As shown in Figure 2E and S11, these layers are bonded to each other through the crosslinks of $Na^+$-binding ligands only through the C–H···π interactions (2.88 Å). Such weak bonding may result in the spacings between the ionic portions of the molecular system that is probably indicative of the crystal morphology being belt-like (Figure S5).

Unfortunately, we could not yet obtain the single crystal of $[Au_{25}(2\text{-}PyET)_{18}]^-\cdot Na^+$ clusters. When the $Au_{25}$ clusters were capped by 2-PyET ligands, the asymmetry of the ortho-substituted Py-group and absence of the aforementioned crosslinks between the adjacent layers probably hindered the crystallization of $[Au_{25}(2\text{-}PyET)_{18}]^-\cdot Na^+$ clusters. However, based on the close similarity in optical (Figure 1) and $^1H$-$^1H$ COSY spectra (Figure S12 and 13), $[Au_{25}(4\text{-}PyET)_{18}]^-$ should have a similar geometric structure to that shown in Figure 2B.

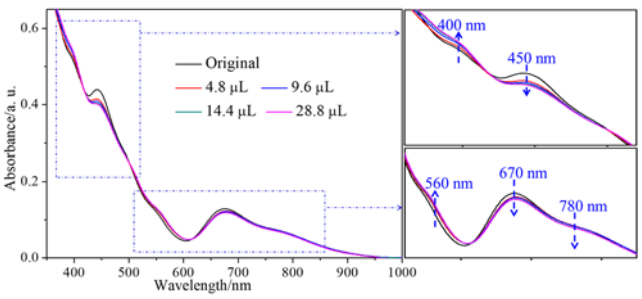


**Figure 3.** UV-vis absorption results obtained for $[Au_{25}(4\text{-}PyET)_{18}]^-$ in MeOH on addition of methanolic HCl (500 mM). The blue arrows denote changes during the protonation.

**Table 1.** Critical $D^+$ concentrations when PyETs were completely protonated in methanol. The data collected are shown in Figures 4 and S20.[a]

| Species | Critical DCl amount (μL) | Critical $D^+$ concentration (M) |
|---|---|---|
| $[Au_{25}(4\text{-}PyET)_{18}]^-$ | ~150 | ~$10.1 \times 10^{-3}$ |
| $[Au_{25}(2\text{-}PyET)_{18}]^-$ | ~130 | ~$8.9 \times 10^{-3}$ |
| Free 4-PyET | ~92 | ~$6.6 \times 10^{-3}$ |
| Free 2-PyET | ~64 | ~$4.8 \times 10^{-3}$ |

[a] The masses for titrations of free PyET ligands were same as the corresponding PyET on $[Au_{25}(PyET)_{18}]^-$ surfaces.

$$[Au_{25}(PyET)_{18}]^- + x\ H^+ \leftrightharpoons [Au_{25}(PyET)_{18-x}(PyET\cdot H^+)_x]^{x-1} \quad (0 \le x \le 18) \qquad (1)$$

Protonation of the Py-group gives rise to the acidic form $-C_5H_4NH^+$. In the case of $[Au_{25}(PyET)_{18}]^-$ clusters, the pendant Py moiety, peripherally exposed to the solution, should also show the protonation characteristics, as depicted by reaction (1). In the $[Au_{25}(4\text{-}PyET)_{18}]^-$–MeOH solution, different amounts of the HCl–MeOH solution (500 mM) were added (see the Experimental section) and the process was first monitored using UV-vis absorption (Figure 3). The intensities of the peaks at ~400 and 560 nm showed a slight increase whereas the peaks at ~450, 670, and 780 nm showed a slight decrease in intensity on protonation. Such absorption changes were also observed when the $Au_{25}(2\text{-}PyET)_{18}$ clusters were treated with $H^+$ except that the amount of HCl required for complete protonation of $[Au_{25}(2\text{-}PyET)_{18}]^-$ clusters (9.6 μL, Figure S14) was lower than that for $[Au_{25}(4\text{-}PyET)_{18}]^-$ clusters (14.4 μL, Figure 3). In addition, $[Au_{25}(PyET)_{18-x}(PyET\cdot H^+)_x]^{x-1}$ ($x$ = 2−4, Figure S15) was detected in the $[Au_{25}(4\text{-}PyET)_{18}]^-$ sample when HCl was added. These spectral changes reveal that $[Au_{25}(PyET)_{18}]^-$ clusters can conjugate with $H^+$ through the pendant Py moiety, similar to the pyridine molecule.

Inspired by the $^1H$-NMR titration of heterocyclic bases,[11a] we further monitored the protonation reaction in $[Au_{25}(PyET)_{18}]^-$ clusters by NMR chemical shifts (see the Experimental section), which were conducted by adding a 16 μL aliquot of DCl-$D_2O$ (50 mM) into 0.6 mL of methanol-$d_4$ containing 0.13 μmol $Au_{25}$ clusters. Here, we focused on the region of the Py moiety ($-C_5H_4N$) in the NMR spectra (see the full ranges in Figure S16 and detailed assignments in Table S4). Under DCl titration, the proton peaks in the $-C_5H_4N\cdots H^+$ group shifted further downfield compared to those of the original clusters in both 4-PyET- and 2-PyET-capped clusters (Figure S17), similar to those of the free PyET (Figure S18–20 and Table S5). The chemical shifts (δ) of pendant Py protons are summarized in Figure 4, which shows that the peak changes depended on the degree of protonation, same as the heterocyclic bases.[11a] It is worth noting that the $D^+$-binding affinity for $[Au_{25}(4\text{-}PyET)_{18}]^-$ clusters (critical $D^+$ concentration: ~$10.1 \times 10^{-3}$ M; Table 1) is weaker than that for $[Au_{25}(2\text{-}PyET)_{18}]^-$ clusters (~$8.9 \times 10^{-3}$ M). This corresponds well to the trend noted in the binding affinities between the NC species and HCl amounts of

complete protonation in UV-vis monitoring (14.4 μL for $[Au_{25}(4\text{-}PyET)_{18}]^-$ against 9.6 μL for $[Au_{25}(2\text{-}PyET)_{18}]^-$; Figures 3 and S12). Moreover, the $H^+$-binding affinities for $Au_{25}$ clusters were clearly weaker than those of free PyET (~6.6 × $10^{-3}$ M for 4-PyET; ~4.8 × $10^{-3}$ M for 2-PyET), which is understandable since the $Au_{25}$ clusters resembled a more rigid macromolecule than the free PyET.[12] In addition, the protons of outer ligands exhibited faster changes than the inner ones, which is ascribed to them being more easily accessible to the external environment.

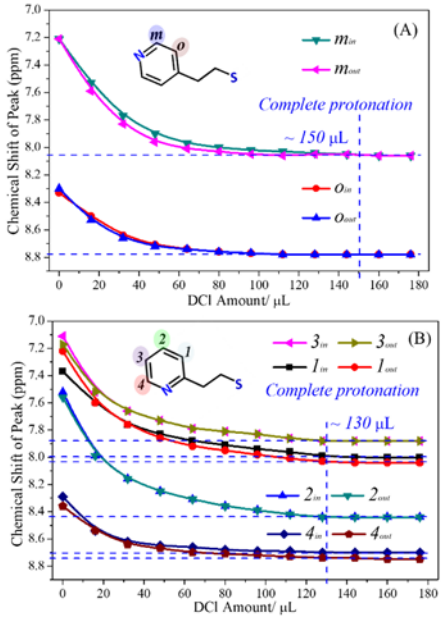


**Figure 4.** $^1$H-NMR chemical shifts in ppm for Py protons in (A) $[Au_{25}(4\text{-}PyET)_{18}]^-$ and (B) $[Au_{25}(2\text{-}PyET)_{18}]^-$ as a function of amount of DCl. The subscripts "*in*" and "*out*" represent two different chemical environments for the 18 PyET ligands, i.e., inner PyET and outer PyET, respectively, that are present in a ratio of 2:1.

Finally, the UV-vis absorption and $^1$H-NMR changes observed for the $[Au_{25}(PyET)_{18}]^-$ clusters were found to be completely reversible when the spectra of the protonated clusters reverted to their original patterns upon neutralization of the solution on the addition of a base such as NaOH or NaOD, as shown in Figure S21. Furthermore, depending on the (de)protonation equilibria, the $[Au_{25}(PyET)_{18}]^-$ clusters unexpectedly showed tunable solubility in aqueous and some organic solvents, as summarized in Table S6. As an example, as demonstrated in Figure S22, deprotonated $[Au_{25}(2\text{-}PyET)_{18}]^-$ clusters were soluble in DCM but insoluble in $H_2O$; on the addition of aqueous HCl, the protonated clusters transferred to the $H_2O$ phase. When further aqueous NaOH was added, it deprotonated the Py moiety and resulted in reversible transfer to the DCM phase.

In conclusion, high-purity $[Au_{25}(SCH_2CH_2Py)_{18}]^-$ clusters protected by a basic pyridyl–thiolate ligand were successfully synthesized for the first time. ESI-MS, single-crystal XRD, and $^1$H-$^1$H COSY characterization indicated that the $[Au_{25}(PyET)_{18}]^-\cdot Na^+$ clusters have a typical core–shell configuration but the $Na^+$ counterion resulted in apparent extension of the exterior ligand shell and a layered crystallographic arrangement in the $[Au_{25}(4\text{-}PyET)_{18}]^-\cdot Na^+$ crystal. UV-vis absorption and $^1$H-NMR results verified that $[Au_{25}(PyET)_{18}]^-$ clusters can conjugate to $H^+$ through the pendant Py moiety, similar to a heterocyclic base. On controlling the $H^+$ involvement, $[Au_{25}(PyET)_{18}]^-$ Clusters showed reversible solubility in aqueous and some organic solvents. This paper, therefore, proposes a new family of basic metalloid clusters. We believe such basic Py-terminated feature will broaden the biological applications of $Au_m(SR)_n$ clusters, such as antimicrobial, in vivo/in vitro biodistribution, photothermal therapy and others.[4] Moreover, the $H^+$-dependent solubility envisions their great potential as catalysts for novel biphasic reactions[13] to facilitate the recovery and recycling of clusters, and in pharmaceutics where self-assembled nanoparticles such as polyelectrolyte complexes with pH-tunable solubility[14] are under intensive research as biocompatible materials and drug/gene delivery systems.

## Acknowledgements

We specially acknowledge Dr. Norihito Fukui (Nagoya Univ.) for his generous assistance on single-crystal X-ray diffraction measurements and analyses, and Mr. Shilei Zhu (Hokkaido Univ.) for his help on crystallization works. Y.I. acknowledges financial support from JSPS KAKENHI grant number 18K14070, Kurata Grant awarded by the Hitachi Global Foundation, Mayekawa Houonkai Foundation, Nippon Sheet Glass Foundation for Materials Science and Engineering, The Kao Foundation for Arts and Sciences, The Suhara Memorial Foundation, TOKUYAMA Science Foundation, The Iwatani Naoji Foundation, Japan Prize Foundation, and Foundation for Interaction in Science & Technology. Partial financial support by KAKENHI (18H01820, 18K22094 to T.Y.) from JSPS is gratefully acknowledged.

### Author Contributions

Y.I. designed the project, Z.H. Y.I. and performed all experiments and analyses, T.Y. participated in the supervision of the project. Z.H. and Y.I. wrote the manuscript, and all authors have reviewed and given approval to the final version of the manuscript.

**Keywords:** pyridyl • gold • clusters • basic • protonation

[1] a) R. Jin, C. Zeng, M. Zhou, Y. Chen, *Chem. Rev.* **2016**, *116*, 10346–10413; b) I. Chakraborty, T. Pradeep, *Chem. Rev.* **2017**, *117*, 8208–8271; c) S. Hossain, Y. Niihori, L. V. Nair, B. Kumar, W. Kurashige, Y. Negishi, *Acc. Chem. Res.* **2018**, *51*, 3114–3124; d) A. W. Cook, T. W. Hayton, *Acc. Chem. Res.* **2018**, *51*, 2456–2464; e) A. Schnepf, H. Schnöckel, *Angew. Chem. Int. Ed.* **2002**, 41, 3532–3554; f) H. Schnöckel, *Chem. Rev.* **2010**, 110, 4125–4163; g) S. Kenzler, C. Schrenk, A. Schnepf, *Angew. Chem. Int. Ed.* **2017**, *56*, 393–396; h) A. Schnepf, *Struct. Bond.* **2017**, 174, 135–200; i) S. Kenzler, F. Feter, C. Schrenk, N. Pollard, A. R. Frojd, A. Z. Clayborne, A. Schnepf, *Angew. Chem. Int. Ed.* **2019**, 58, 5902–5905.

[2] a) G. Li, R. Jin, *Acc. Chem. Res.* **2013**, *46*, 1749–1758; b) X. K. Wan, J. Q. Wang, Z. A. Nan, Q. M. Wang, *Sci. Adv.* **2017**, *3*, e1701823; c) G. Li, H. Abroshan, C. Liu, S. Zhuo, Z. Li, Y. Xie, H. J. Kim, N. L. Rosi, R. Jin, *ACS Nano* **2016**, *10*, 7998–8005.

[3] a) G. Guan, S. Y. Zhang, Y. Cai, S. Liu, M. S. Bharathi, M. Low, Y. Yu, J. Xie, Y. Zheng, Y. W. Zhang, M. Y. Han, *Chem. Commun.* **2014**, *50*,

5703–5705; b) R. Shen, P. Liu, Y. Zhang, Z. Yu, X. Chen, L. Zhou, B. Nie, A. Żaczek, J. Chen, J. Liu, *Anal. Chem.* **2018**, *90*, 4478–4484; c) Y. Teng, X. Jia, J. Li, E. Wang, *Anal. Chem.* **2015**, *87*, 4897–4902.

[4] a) L. Polavarapu, M. Manna, Q. H. Xu, *Nanoscale* **2011**, *3*, 429–434; b) K. Zheng, M. I. Setyawati, D. T. Leong, J. Xie, *Chem. Mater.* **2018**, 30, 2800–2808; c) K. Zheng, M. I. Setyawati, D. T. Leong, J. Xie, *ACS Nano* **2017**, 11, 6904–6910.

[5] a) Y. Chen, C. Zeng, D. R. Kauffman, R. Jin, *Nano Lett.* **2015**, *15*, 3603–3609; b) C. Zeng, T. Li, A. Das, N. L. Rosi, R. Jin, *J. Am. Chem. Soc.* **2013**, *135*, 10011–10013; c) C. Zeng, C. Liu, Y. Pei, R. Jin, *ACS Nano* **2013**, *7*, 6138–6145; d) C. Zeng, Y. Chen, K. Kirschbaum, K. Appavoo, M. Y. Sfeir, R. Jin, *Sci. Adv.* **2015**, *1*, e1500045.

[6] a) J. Yan, B. K. Teo, N. Zheng, *Acc. Chem. Res.* **2018**, *51*, 3084–3093; b) T. Higaki, Q. Li, M. Zhou, S. Zhao, Y. Li, S. Li, R. Jin, *Acc. Chem. Res.* **2018**, *51*, 2764–2773; c) C. J. Ackerson, P. D. Jadzinsky, R. D. Kornberg, *J. Am. Chem. Soc.* **2005**, 1*27*, 6550–6551; d) S. Knoppe, T. Bürgi, *Acc. Chem. Res.* **2014**, *47*, 1318–1326; e) Z. Wu, C. Gayathri, R. R. Gil, R. Jin, *J. Am. Chem. Soc.* **2009**, *131*, 6535–6542; f) H. Yang, Y. Wang, J. Lei, L. Shi, X. Wu, V. Makinen, S. Lin, Z. Tang, J. He, H. Hakkinen, L. Zheng, N. Zheng, *J. Am. Chem. Soc.* **2013**, *135*, 9568–9571; g) J. Z. Yan, J. Zhang, X. M. Chen, S. Malola, B. Zhou, E. Selenius, X. M. Zhang, P. Yuan, G. C. Deng, K. L. Liu, H. F. Su, B. K. Teo, H. Hakkinen, L. S. Zheng, N. F. Zheng, *Natl. Sci. Rev.* **2018**, *5*, 694–702; h) Z. Wu, R. Jin, *Nano Lett.* **2010**, *10*, 2568–2573; i) X. Yuan, N. Goswami, W. Chen, Q. Yao, J. Xie, *Chem. Commun.* **2016**, *52*, 5234–5237; j) X. Kang, M. Zhu, *Chem. Soc. Rev*. **2019**, *48*, 2422–2457; k) C. Lavenn, A. Demessence, A. Tuel, *Catal. Today* **2014**, *235*, 72–78; l) C. J. Ackerson, P. D. Jadzinsky, G. J. Jensen, R. D. Kornberg, *J. Am. Chem. Soc.* **2006**, *128*, 2635–2640.

[7] a) C. Lavenn, F. Albrieux, G. Bergeret, R. Chiriac, P. Delichere, A. Tuel, A. Demessence, *Nanoscale* **2012**, *4*, 7334–7337; b) X. Yuan, B. Zhang, Z. Luo, Q. Yao, D. T. Leong, N. Yan, J. Xie, *Angew. Chem., Int. Ed.* **2014**, *53*, 4623–4627; c) M. M. Hoque, D. M. Black, K. M. Mayer, A. Dass, R. L. Whetten, *J. Phys. Chem.* Lett. **2019**, 10, 3307–3311; d) M. M. Hoque, A. Dass, K. M. Mayer, R. L. Whetten, *J. Phys. Chem. C* **2019**, 123, 14871–14879.

[8] a) Y. Ishida, K. Narita, T. Yonezawa, R. L. Whetten, *J. Phys. Chem. Lett.* **2016**, *7*, 3718–3722; b) Y. Ishida, Y. L. Huang, T. Yonezawa, K. Narita, *ChemNanoMat* **2017**, *3*, 298−302; c) Z. Huang, Y. Ishida, K. Narita, T. Yonezawa, *J. Phys. Chem. C* **2018**, *122*, 18142−18150; d) Y. Ishida, R. D. Corpuz, T. Yonezawa, *Acc. Chem. Res.* **2017**, *50*, 2986–2995.

[9] a) J. F. Parker, J. E. Weaver, F. McCallum, C. A. Fields−Zinna, R. W. Murray, *Langmuir* **2010**, *26*, 13650−13654; b) M. Zhu, C. M. Aikens, F. J. Hollander, G. C. Schatz, R. Jin, *J. Am. Chem. Soc.* **2008**, *130*, 5883−5885; c) S. Kumar, R. Jin, *Nanoscale* **2012**, *4*, 4222−4227; d) Y. Negishi, K. Nobusada, T. Tsukuda, *J. Am. Chem. Soc.* **2005**, *127*, 5261−5270; e) M. W. Heaven, A. Dass, P. S. White, K. M. Holt, R. W. Murray, *J. Am. Chem. Soc.* **2008**, *130*, 3754−3755.

[10] R. D. Hancock, *Chem. Soc. Rev.* **2013**, *42*, 1500−1524.

[11] a) A. D. Gift, S. M. Stewart, P. Kwete Bokashanga, *J. Chem. Educ.* **2012**, *89*, 1458−1460; b) A. Venzo, S. Antonello, J. A. Gascón, I. Guryanov, R. D. Leapman, N. V. Perera, A. Sousa, M. Zamuner, A. Zanella, F. Maran, *Anal. Chem.* **2011**, *83*, 6355−6362; c) H. Qian, M. Zhu, C. Gayathri, R. R. Gil, R. Jin, *ACS Nano* **2011**, *5*, 8935−8942.

[12] J. Koivisto, X. Chen, S. Donnini, T. Lahtinen, H. Häkkinen, G. Groenhof, M. Pettersson, *J. Phys. Chem. C* **2016**, *120*, 10041−10050.

[13] a) I. T. Horváth, J. Raba, *Science* **1994**, *266*, 72−75; b) R. M. Crooks, M. Zhao, L. Sun, V. Chechik, L. K. Yeung, *Acc. Chem. Res.* **2001**, *34*, 181−190.

[14] a) Z. Sui, J. A. Jaber, J. B. Schlenoff, *Macromolecules* **2006**, *39*, 8145−8152; b) Q. Zhao, D. W. Lee, B. K. Ahn, S. Seo, Y. Kaufman, J. N. Israelachvili, J. H. Waite, *Nat. Mater.* **2016**, *15*, 407−412; c) J. E. Laaser, E. Lohmann, Y. Jiang, T. M. Reineke, T. P. Lodge, *Macromolecules* **2016**, *49*, 6644−6654.

# COMMUNICATION

**X-ray structure of basic $[Au_{25}(SCH_2CH_2Py)_{18}]^-$ cluster**: The structure is similar to that known for the phenyl ethanethiolate analog, but with pyridyl-N coordination to $Na^+$, a more relaxed ligand shell, and a profoundly layered arrangement in solid state. This paper paves the way to realize a new family of metal clusters possessing basic properties.

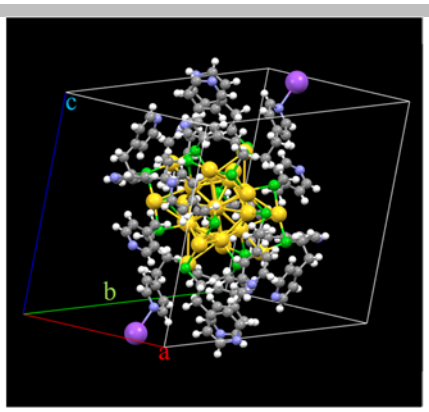


*Zhong Huang, Yohei Ishida,* and Tetsu Yonezawa**

***Page No. – Page No.***

**Basic $[Au_{25}(SCH_2CH_2Py)_{18}]^-$ Clusters: Synthesis, Layered Crystallographic Arrangement, and Unique Surface Protonation**